A Monte-Carlo Study of Classical Spectral Estimation of the Backscatter in K-distributed Images

Oscar H. Bustos[1], Ana G. Flesia[1], Alejandro C. Frery[2]

[1]Fa.M.A.F–Facultad de Matemática Astronomía y Física, Ciudad Universitaria, 5000 Córdoba, Argentina
bustos,flesia@mate.uncor.edu
[2]Departamento de Informática, Universidade Federal de Pernambuco, Recife, PE, Brazil
frery@di.ufpe.br

Abstract. Some estimators for the spectral density of the return in Synthetic Aperture Radar (SAR) images are studied using Monte Carlo experiences. The spectral density is an important quantifier of the texture that, in turn, can be related to biophysical magnitudes and it can be used to establish the kind of target being observed. These images are contaminated by a particular kind of noise, called speckle, that departs from the classical hypothesis of obeying the Gaussian law and of entering the signal in an additive manner requiring, thus, a careful treatment. The departure from the Gaussian law will be modeled here by means of the K distribution. This law arises from certain (very realistic) hypothesis for the relationship between signal and noise. The empirical observation of structured data is modeled by the use of spatial correlation. There are two approaches to the problem of the presence of speckle noise, one being the use of techniques for its reduction (usually specially devised filters) and the other the proposal of methodologies that take its presence into account. These approaches will be compared here, to the problem of estimating the spatial correlation structure of the ground truth. The performance of these estimators will be assessed using Monte Carlo experiences, since the problem is analytically intractable.

1 Introduction

An imaging radar is a system for earth observation based on an emitting and receiving device that operates in the range of microwaves. The system sends a pulse of electromagnetic energy, the targets reacts to this stimulus and, eventually, part of this energy is returned to the system. This return signal, if available, is processed on order to infer about the properties of the target.

Imaging radar systems constitute a major advance in remote sensing, since they allow the obtainment of dielectric properties of targets independently of the availability of natural illumination (they carry their own source of energy) and of the weather conditions (microwaves are unaffected, to a great extent, by clouds, fog, rain, smog etc.). Besides these desirable properties, the frequency of the signal employed is able to penetrate canopy and other masses.

The term *synthetic* refers to the fact that larger antennas and, thus, greater resolutions, are obtained with processing techniques. These characteristics allow the use of synthetic aperture radar (SAR) systems for continuous earth monitoring.

The statistical properties here presented are common to every image generated with coherent illumination, as is the case of ultrasound, laser and sonar.

The relevant information present in these images is concentrated in the mean cross section. This quantity is sensitive to many parameters that characterize the target, as dielectric constant and surface roughness, among other. Each individual cell in the image (pixel) has this information, but it is corrupted by the *speckle* noise, which is due to interference phenomena in the reflected signal.

The purpose of this work is the assessment of the effect of speckle noise in the ability to infer the properties of the targets, more specifically, to estimate the spatial correlation structure through the estimation of the spectrum. The spatial correlation of the image data is a very important feature, since it allows the discrimination among different types of targets, and it is required for some noise reduction techniques (see [5]).

In this paper we shall test in a controlled clutter environment the performance of some cross section power spectrum estimators, which have been already presented in [1]. This estimators are based on classical estimates of the return and noise spectrum, like sample periodogram and smoothed sample periodogram, so we shall study the performance of these estimates based on the performance of the other estimates involved in making them. An accurate evaluation of the error in the estimation is analytically too difficult to be performed in the general case. Accordingly, we present

a comparison among four estimators based on simulation.

2 The Multiplicative Model for SAR Images

The model for SAR images here presented is the one studied in [6, 9].

Consider $(s_1, s_2) \in \mathbf{Z}^2$, a two-dimensional vector representing the position (azimuth and range) in the discrete domain. When an electromagnetic wave is sent towards the position (s_1, s_2), the physical properties of the target cause changes in the phase of the signal $\phi(s_1, s_2)$ and in its amplitude $A(s_1, s_2)$. The SAR system observes in every coordinate the pair of values $(A\cos(\phi), A\sin(\phi))$, weighted by its point spread function. This complex number has information about the mean cross section σ, masked by the speckle noise.

The parameter σ may be constant across the target (as is the case in many crops and grass areas), or it may fluctuate (as in forests). This pixel-to-pixel variation defines the concept of *texture* for SAR images. A possible way to characterize this information is considering the values of σ as the outcome of a stochastic process. The usual texture measures in this context are the density and some higher order moments of the process.

Let us now define the process $S : \Omega \to \mathbf{C}^{\mathbf{Z}^2}$, that represents the complex reflectivity in every resolution cell, i.e., each outcome $\{S(\omega)\}_{\mathbf{Z}^2}$ of the process denotes the possible amplitude and phase fluctuations caused by the aforementioned interference phenomena.

The relationship between data and noise is, for SAR images (see [8]), multiplicative and, thus, can be stated as $S = X \cdot Y$, where $X : \Omega \to \mathbf{R}^{\mathbf{Z}^2}$ represents the amplitude of the returned signal (given by $X = \sqrt{\sigma}$), and the complex process $Y : \Omega \to \mathbf{C}^{\mathbf{Z}^2}$ models the speckle noise. Independence can be assumed between X and Y. Additional hypothesis are

1. The processes X and Y are statistically stationary, at least to the second order.

2. The process Y is a white noise.

For the validity of the first hypothesis it is essential to have $E(\sigma_{\mathbf{s}}) = \alpha$ for every $\mathbf{s} \in \mathbf{Z}^2$, i.e., the expected value of the mean backscatter is assumed constant.

3 Intensity multilook format

A very convenient real process, namely $Z = |S|^2$ can be constructed from the complex reflectivity S. Therefore, $Y_I = |Y|^2$ will denote the intensity speckle, and using the multiplicative model one has $Z = \sigma Y_I$.

The complex format has more information than the intensity one [2, 9], but these format is available for a limited number of sensors.

A simple method for speckle noise reduction is the multilook format, which consists of taking the mean over n (ideally independent) samples of the same random process. Assuming that the r-th observation is $S_{r,(s_1,s_2)} = (X \cdot Y_r)(s_1, s_2)$, if $1 \leq r \leq n$, then the n-looks signal is given by $\overline{S} = \sigma \overline{Y_I}$, where $\overline{Y_I}$ is the mean of n observations of the speckle process, corresponding to n different images and where it is assumed that the outcome of X does not vary in these n images.

Though the number of looks n should be, in principle, an integer this is seldom the case since the observations are, in practice, not independent. Its estimation is studied in [10].

4 Distributions for rough targets

Assuming valid the multiplicative model, the complex return from each pixel can be written as $S = \sqrt{\sigma}Y$. Speckle in complex format has bivariate Gaussian distribution, with zero mean and covariance matrix

$$\left[\begin{array}{cc} 1/2 & 0 \\ 0 & 1/2 \end{array} \right],$$

so the real and imaginary components are independent and equally distributed. Under this assumption the intensity speckle Y_i obeys an exponential law with unitary mean.

Since multilook images are formed taking the mean over n independent samples, multilook speckle obeys a $\Gamma(n, n)$ law, with density

$$g_{Y_I}(y) = \frac{n^n}{\Gamma(n)} y^{n-1} \exp(-y/n) \quad y, n > 0.$$

The mean cross section that characterizes rough targets can be modeled by another Γ distribution, with density given by

$$g_\sigma(\sigma) = \frac{\beta^\nu}{\Gamma(\nu)} \sigma^{\nu-1} \exp(-\sigma/\beta), \quad \sigma, \nu, \beta > 0,$$

whose expected value is $\frac{\nu}{\beta}$, and where ν and β are called shape and scale parameters, respectively.

The adequacy of this model has been extensively assessed from both the theoretical and empirical points of view.

Many applications assume that the process σ obeys the $\Gamma(\nu, \beta)$ distribution in every coordinate, and that distinct positions are independent. In this work the assumption of independence will be replaced by a more realistic model of spatial correlation.

Amongst the many available ways to incorporate spatial correlation, a weak stationary process will be assumed here. In doing so, it is necessary to adopt a characterization for the process, since the product of the marginal densities is no longer a valid extension.

To be consistent with the Γ model assumed for the marginal data, a family of correlated Γ random variables should be used but, differently from the Gaussian case, there is no unique characterization of such model.

5 Periodic model for SAR images and spectral estimation

Some properties of the spectrum will be studied here and, for this task, it is convenient to assume that the image or sub image under study is a sample from a periodic two dimensional signal that has been corrupted by speckle noise in a multiplicative manner, as previously presented.

Let us recall that a two dimensional stochastic process Z is said periodic if $U(s_1,s_2) = U(s_1+N_1,s_1) = U(s_1,s_2+N_2)$ in every $(s_1,s_2) \in \mathbf{Z}^2$, where N_1 and N_2 are positive integers. If these are the smallest possible numbers such that the property holds, then they are called the *horizontal* and *vertical periods*, respectively. It is easy to see that every periodic array with horizontal and vertical periods N_1 and N_2 is completely specified by $N_1 N_2$ convenient values, which lie in the region

$$R_{N_1 N_2} = \{\mathbf{s} : 0 \leq s_1 \leq N_1 - 1, 0 \leq s_2 \leq N_2 - 1\},$$

namely the fundamental period. In this work, the horizontal and vertical periods will be equal, $N_1 = N_2 = N$, so we will refer to the correspondent fundamental period by R_N.

Let σ, Y and Z be periodic, non-negative stochastic process, each with fundamental period R_N, such that they obey the multiplicative model $Z(s_1,s_2) = \sigma(s_1,s_2)Y(s_1,s_2)$. We will assume that σ models the terrain mean cross section, that Y is the n-look intensity speckle and that Z is the n-look intensity return image.

Notice that if U is any periodic process then for each coordinate $(s_1,s_2) \in R_N$ the *Fourier coefficient* of U in (s_1,s_2), is given by

$$\hat{U}_{(s_1,s_2)} = \frac{1}{N^2} \sum_{k_1=0}^{N-1} \sum_{k_2=0}^{N-1} U_{(k_1,k_2)} \omega^*_{s_1 k_1, N} \omega^*_{s_2 k_2, N}$$

for every $0 \leq s_1, s_2 \leq N - 1$ and $\omega_{k,N} = \exp(\frac{2\pi k}{N})$. The function $\hat{U}$ is called *Fourier series* of U.

In [1] it is proved that if U is a stochastic two-dimensional weakly stationary process, i.e., if for every $(s_1,s_2),(t_1,t_2) \in \mathbf{Z}^2$ holds that

1. $E(U_{(s_1,s_2)}) = \mu_U$ and that

2. $E(U_{(s_1,s_2)}.U_{(t_1,t_2)}) = R_U(s_1 - t_1, s_2 - t_2)$

then the power spectrum of U is the function S_U that satisfies

$$
\begin{aligned}
S_U(s_1,s_2) &= \\
&= E(\hat{U}(s_1,s_2)^* \hat{U}(s_1,s_2)) \\
&= \frac{1}{N^2} \sum_{k_1=0}^{N-1} \sum_{k_2=0}^{N-1} R_U(k_1,k_2) \omega_{k_1 s_1, N} \omega_{k_2 s_2, N},
\end{aligned}
$$

for every $0 \leq s_1, s_2 \leq N - 1$, where $*$ denotes the complex conjugate.

It is also proved that if the process Y that models the speckle noise is a two-dimensional uncorrelated stochastic periodic n-looks white noise process, then

$$S_\sigma(s_1,s_2) = \frac{1}{n^2} \left[S_Z(s_1,s_2) - \frac{1}{1+n}\overline{S_Z} \right]$$

where

$$\overline{S_Z} = \frac{1}{N^2} \sum_{k_1=0}^{N-1} \sum_{k_2=0}^{N-1} S_Z(k_1,k_2).$$

From this we conclude that it is possible to estimate S_σ using estimators for S_Z.

This paper expands this earlier results, in the following directions:

1. an accurate clutter simulation with specified correlation properties, based on correlated Gamma vectors, will be obtained;

2. using this fields as input data, a comparison between the performance of estimators of S_σ will be achieved.

The estimators of S_Z that we will work with are the sample periodogram, and the sample periodogram smoothed with two windows, the Tuckey-Hanning and the Hamming ones. These estimators will be applied to both raw (unprocessed) and filtered data.

6 Correlated Gamma distribution

Assume U is a weakly stationary stochastic process with fundamental period R_N, and non trivial auto-covariance function. The definition of a random process with correlated Gamma distribution is not an easy task, since there no unique definition. In this work, the definitions presented [7] will be used.

Definition 6.1 *A random vector U' is said to have a correlated Gamma distribution if each component obeys a Gamma law.*

Definition 6.2 *A stochastic process is said to have a correlated Gamma distribution if any subset of variables of the process, seen as a vector, has correlated Gamma distribution.*

7 Multivariate Reduction Method

This method allows the obtainment of a random field with marginal Γ distributions with shape parameter $\nu = m/2$, m integer, but this limitation is of no practical effect for the applications we bear in mind: SAR images [10]. It is based on the generation of Gaussian fields, independent among them but with a certain correlation inner structure. Once these fields are simulated, the values among corresponding co-ordinates are squared and added. In this work it is of particular interest the generation of a particular correlation structure: that induced by the filtering with a mask.

Definition 7.1 *Consider the periodic function E with fundamental period R_N given by*

$$E(s_1, s_2) = \begin{cases} \exp(-\frac{1}{2}\frac{s_1^2+s_2^2}{l^2})) & \text{if } \mathbf{s} \in R_1 \\ \exp(-\frac{1}{2}\frac{(N-s_1)^2+s_2^2}{l^2}) & \text{if } \mathbf{s} \in R_2 \\ \exp(-\frac{1}{2}\frac{s_1^2+(N-s_2)^2}{l^2}) & \text{if } \mathbf{s} \in R_3 \\ \exp(-\frac{1}{2}\frac{(N-s_1)^2+(N-s_2)^2}{l^2}) & \text{if } \mathbf{s} \in R_4 \end{cases}$$

where $R_1 = \{\mathbf{s} = (s_1, s_2) : 0 \le s_1, s_2 \le \frac{N}{2}\}$, $R_2 = \{\mathbf{s} : \frac{N}{2}+1 \le s_1 \le N-1, 0 \le s_2 \le \frac{N}{2}\}$, $R_3 = \{\mathbf{s} : 0 \le s_1 \le \frac{N}{2}, \frac{N}{2}+1 \le s_2 \le N-1\}$, and $R_4 = \{\mathbf{s} : \frac{N}{2}+1 \le s_1, s_2 \le N-1\}$.

Consider also $E_1 : \mathbf{Z} \to \mathbf{R}$ the one-dimensional function with period $R = \{0, \ldots, N-1\}$ given by

$$E_1(j) = \begin{cases} \exp(-\frac{1}{2}\frac{j^2}{l^2}) & 0 \le j \le \frac{N}{2} \\ \exp(-\frac{1}{2}\frac{(N-j)^2}{l^2}) & \frac{N}{2}+1 \le j \le N-1 \end{cases} \tag{1}$$

Note that E is a separable function, i.e., for every $(s_1, s_2) \in R_N$ holds that $E(s_1, s_2) = E_1(s_1) \cdot E_1(s_2)$.

It can be seen that the Fourier transform of E_1, $\hat{E}_1(s_1) = N^{-1}\sum_{k=0}^{N-1} E_1(k)\omega_{s_1 k, N}^*$, is a positive real function, so it has one and only one square root.

Definition 7.2 *Let $\theta_1 : \mathbf{Z} \to \mathbf{R}$ be the function defined by $\theta_1(s_1) = \sum_{k=0}^{N-1}\sqrt{\hat{E}_1(k)}\omega_{ks_1, N}$ with period $R = \{0, \ldots, N-1\}$, and let $\theta : \mathbf{Z}^2 \to \mathbf{R}$ be the periodic function with fundamental period R_N given by $\theta(s_1, s_2) = \theta_1(s_1)\theta_1(s_2)$.*

It holds that

$$\theta * \theta(s_1, s_2) = \sum_{t_1=0}^{N-1}\sum_{t_2=0}^{N-1} \theta(t_1, t_2)\theta(s_1 - t_1, s_2 - t_2)$$
$$= E(s_1, s_2),$$

where

$$\theta(s_1, s_2) = \begin{cases} \theta(N - s_1, s_2) & \text{if } \mathbf{s} \in R_2 \\ \theta(s_1, N - s_2) & \text{if } \mathbf{s} \in R_3 \\ \theta(N - s_1, N - s_2) & \text{if } \mathbf{s} \in R_4 \end{cases}$$

Definition 7.3 *Let ζ_k with $1 \le k \le 2\nu$, be independent periodic white noise Gaussian stochastic processes with fundamental period R_N. Consider also the periodic processes ξ_k, $1 \le k \le 2\nu$, with fundamental period R_N defined by*

$$\xi_k(s_1, s_2) = (\theta * \zeta_k)(s_1, s_2)$$
$$= \sum_{t_1=0}^{N-1}\sum_{t_2=0}^{N-1}\zeta_k(t_1, t_2)\theta(s_1 - t_1, s_2 - t_2)$$

Note that the processes ξ_k defined above satisfy the following properties

1. they are marginally formed by Gaussian random variables, since $\xi_k(s_1, s_2) \sim N(0, \frac{1}{2}(\theta * \theta)(0, 0))$;

2. $E(\xi_k(0,0)\xi_k(s_1, s_2)) = \frac{1}{2}(\theta * \theta)(s_1, s_2) = \frac{1}{2}E(s_1, s_2)$.

3. $\rho(\xi(0, 0), \xi(s_1, s_2)) = E(s_1, s_2)$

Definition 7.4 *Let η be the periodic stochastic process with fundamental period R_N defined by*

$$\eta(s_1, s_2) = \sum_{k=1}^{2\nu}\xi_k^2(s_1, s_2) \qquad \forall (s_1, s_2) \in R_N,$$

and also consider $\beta > 0$. Define, for every $(s_1, s_2) \in R_N$, the stochastic process σ by $\sigma(s_1, s_2) = \beta\eta(s_1, s_2)$.

The following statements hold:

1. The stochastic process η is periodic, weakly stationary with correlated distribution and $\eta(s_1, s_2) \sim \Gamma(\nu, 1)$.

2. The stochastic process σ is periodic, weakly stationary with correlated Gamma distribution such that

   (a) $\sigma_{(s_1, s_2)} \sim \Gamma(\nu, \beta)$, therefore $E(\sigma(s_1, s_2)) = \frac{\nu}{\beta}$ and $Var(\sigma(s_1, s_2)) = \frac{\nu}{\beta^2}$.

   (b) The coefficient of correlation of the process σ is given by $\rho(\sigma_{(s_1, s_2)}, \sigma_{(0,0)}) = E^2(s_1, s_2)$.

   (c) Its normalized auto-correlation function is given by $r_\sigma(s_1, s_2) = 1 + \frac{1}{\nu}E^2(s_1, s_2)$.

   (d) Its auto-correlation function is $R_\sigma(s_1, s_2) = \frac{\nu^2}{\beta^2}(1 + \frac{1}{\nu}E^2(s_1, s_2))$.

   (e) It can be seen that is spectral density function is $S_\sigma(\mathbf{s}) = \frac{1}{N^2}\sum_{\mathbf{k} \in R_N}(k_1, k_2)\omega_{k_1 s_1 + k_2 s_2, N}$.

7.1 Simulation of heterogeneous targets

The aforementioned multivariate reduction method was implemented in the IDL 5.2 development platform for Windows. The algorithm, in pseudo language, is as follows:

1. Generate ζ_k Gaussian white noise fields with variance $1/2$, $1 \leq k \leq \nu$.

2. Define $e_1(j) = \exp(-\frac{1}{2}\frac{j^2}{l^2})$ if $0 \leq j \leq \frac{N}{2}$, and $e_1(j) = e_1(N-j)$ if $\frac{N}{2}+1 \leq j \leq N-1$.

3. Define
$$\psi_2(s_1, s_2) = \sqrt{\mathrm{FFT}(e_1, -1)(s_1).\mathrm{FFT}(e_1, -1)(s_2)}$$

4. Define $\xi_k = \mathrm{FFT}\,(\psi_2.\,\mathrm{FFT}\,(\zeta_k, -1), 1)$, $1 \leq k \leq 2\nu$.

5. Define $\sigma = \frac{1}{\beta}\sum_{k=1}^{2\nu}\xi_k^2$.

6. Generate $Y \sim \Gamma(n, n)$, where n is the number of looks of the final image.

7. Return $Z = \sigma Y$.

In this algorithm $\mathrm{FFT}(U, -1)$ and $\mathrm{FFT}(U, 1)$ represent the direct and inverse Fourier transform, respectively. They are evaluated with a routine based on the Fast Fourier Transform algorithm. The bigger the parameter ν the slower the simulation algorithm will be, since the more correlated Gaussian random fields will have to be generated. The distribution of the product of the independent distributed random variables is known as Intensity K, and it has a central role in SAR image analysis (see, for instance, [2]).

The following images are constructed with four different shapes parameters and four different lengths of correlation. Figure 1 shows sixteen images with Gamma correlated distribution; these are samples of the ground truths to be estimated through the procedures that will be presented in section 8. Figure 2 exhibits sixteen K-correlated images with the same parameters and three numbers of looks. These are samples of the data that will be used by the first three algorithms to be presented in the following section.

8 Sample and smoothed periodograms

If $R_N = \{(s_1, s_2) : 0 \leq s_1, s_2 \leq N-1\}$ with $N = 2^k$, and k integer, we define the set $\mathbf{C}^{R_N} = \{u : R_N \to \mathbf{C}\}$ with the canonical product

$$\langle u, v \rangle = \frac{1}{N^2}\sum_{s_1=0}^{N-1}\sum_{s_2=0}^{N-1}u(s_1, s_2)v(s_1, s_2)^*, \qquad (2)$$
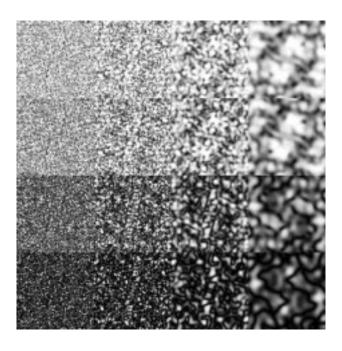

Figure 1: Sixteen Gamma correlated images, with $\nu \in \{0.5, 1, 1.5, 2\}$ varying in the rows and correlation lag $\ell \in \{1, 2, 4, 8\}$ varying in the columns.
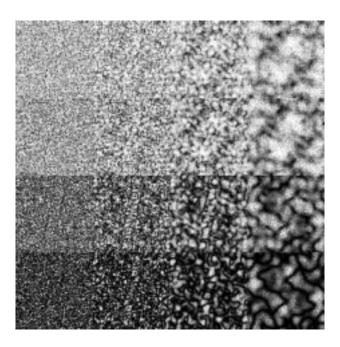

Figure 2: Sixteen K correlated images corresponding to the Gamma correlated fields shown in Figure 1.

for every pair of complex complex matrices $u, v \in \mathbf{C}^{R_N}$. For every $(s_1, s_2) \in R_N$ let $\omega_{(s_1,s_2)} \in \mathbf{C}^{R_N}$ be defined as $\omega_{(s_1,s_2)}(k_1, k_2) = \omega_{k_1 s_1, N} \omega_{k_2, s_2, N}$. It can be proved that

$$\left(\omega_{(0,0)}, \ldots, \omega_{(0, N-1)}, \ldots, \omega_{(N-1,0)}, \ldots, \omega_{(N-1, N-1)} \right)$$

is an ortho-normal basis of $\mathbf{C}^{R_N}$, with respect to the inner product defined in eq. (2), called Fourier basis. Therefore, if $u \in \mathbf{C}^{R_N}$, the Fourier transform is defined as

$$
\begin{aligned}
\hat{u}(s_1, s_2) &= \langle u, \omega_{(s_1,s_2)} \rangle \\
&= \frac{1}{N^2} \sum_{k_1=0}^{N-1} \sum_{k_2=0}^{N-1} u(k_1, k_2) \omega_{(s_1,s_2)}(k_1, k_2)^*.
\end{aligned}
$$

Define the set of frequencies associated to R_N as $\mathcal{F}_N = \{ \lambda(s_1, s_2) = (\frac{2\pi s_1}{N}, \frac{2\pi s_2}{N}) : (s_1, s_2) \in R_N \}$.

Definition 8.1 *The sample periodogram of the complex sequence* $u \in \mathbf{C}^{R_N}$ *is the function* $I_N(u) :\rightarrow [0, +\infty)$ *given by* $I_N(u)(\lambda(s_1, s_2)) = |\hat{u}(s_1, s_2)|^2$.

If U is a weakly stationary stochastic process and $u = U(\omega)$ is a sample of this process, the sample auto-correlation function $r_u : R_N \rightarrow \mathbf{C}$ is defined, for every $s_1, s_2 \in R_N$, as the double summation $r_u(s_1, s_2) = N^{-2} \sum_{k_1=0}^{N-s_1-1} \sum_{k_2=0}^{N-s_2-1} u(k_1, k_2) u(k_1 + s_1, k_2 + s_2)^*$. It can be seen that

$$
\begin{aligned}
I_N(u)(\lambda(s_1, s_2)) &= \\
&= \frac{1}{N^2} \sum_{k_1=0}^{N-1} \sum_{k_2=0}^{N-1} r_{uu}(k_1, k_2) \omega_{(s_1,s_2)}(k_1, k_2),
\end{aligned}
$$

where r_{uu} is a summation of sample auto-correlations, that estimate the auto-correlation of the process $R_U = E(U_{(t_1,t_2)} U^*_{(s_1+t_1, s_2+t_2)})$ in the values of the period R_N. Then, since

$$
\begin{aligned}
S_U(s_1, s_2) &= \\
&= E(|\hat{U}(s_1, s_2)|^2) \\
&= \frac{1}{N^2} \sum_{k_1=0}^{N-1} \sum_{k_2=0}^{N-1} R_U(k_1, k_2) \omega_{(s_1,s_2)}(k_1, k_2)
\end{aligned}
$$

it is possible to estimate this function with $I_N(u)$.

Nevertheless, I_N does not have a good performance close to the edges of R_N, so it is advisable to conveniently weight the observations, and then estimate the periodogram [4]. In other words, instead of working with the observed values $\{ u(s_1, s_2), (s_1, s_2) \in R_N \}$, the weighted data

$$\{ a(s_1, s_2) u(s_1, s_2), (s_1, s_2) \in R_N \}$$

will be used, with

$$a(s_1, s_2) = h(\frac{s_1}{N-1}) h(\frac{s_2}{N-1}),$$

where $h : [0, 1] \rightarrow [0, 1]$, $h(0) = 0$, $h(1) = 1$. Two functions usually found in the literature will be here considered: the Tuckey-Hanning window given by $h_T(s) = \frac{1}{2}(1 - \cos(2\pi s))$, and the Hamming window defined as $h_H(s) = 0.54 - 0.46 \cos(2\pi s)$.

9 Simulation and Results

If $z : R_N \rightarrow \mathbf{R}$ is the image sample under study, obtained by the simulation method previously presented, the following estimators for the spectrum of the underlying process Z will be considered: the sampled periodogram $I_N(z)$, the smoothed periodogram over the Tuckey-Hanning window $I_{N,T}(z)$, and the smoothed periodogram over the Hamming window, $I_{N,H}(z)$. The correspondent estimators of σ are

$$
\begin{aligned}
P_N(\sigma) &= \frac{1}{n^2}\left(I_N(z) - \frac{1}{n+1}\overline{I_N(z)} \right) \\
P_{N,T}(\sigma) &= \frac{1}{n^2}\left(I_{N,T}(z) - \frac{1}{n+1}\overline{I_{N,T}(z)} \right) \\
P_{N,H}(\sigma) &= \frac{1}{n^2}\left(I_{N,H}(z) - \frac{1}{n+1}\overline{I_{N,H}(z)} \right)
\end{aligned}
$$

where n is the number of looks of the image z.

Applying the Lee filter, (see [2, 5]) to z, with a window of size 3×3 the image $\hat{\sigma}$ is obtained. This image is an estimator of the true incorrupted image σ and, therefore, it should be possible to estimate S_σ directly with the sample periodogram $P_{N,F}(\sigma) = I_N(\text{Leefilt}(z))$. The samples shown in Figure 2, after being submitted to this speckle reduction technique, are shown in Figure 3. These are the input data for the estimator $P_{N,F}$, that uses filtered images.

The Lee filter is a local linear minimum mean square error filter, derived from a linearization of the multiplicative model, by Taylor expansion, around the mean. This approximation transforms that model into an additive one, and then the Wiener filter is applied.

These four estimators were implemented in the IDL 5.2 platform, as well as a good approximation of the true power spectral density

$$S_\sigma(s_1, s_2) = \frac{1}{N^2}\text{FFT}(R_\sigma, 1),$$

using the previously mentioned algorithm based on the Fast Fourier Transform.
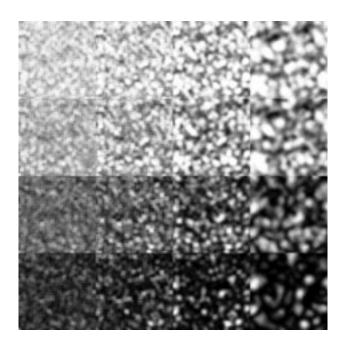
In order to assess the relative performance of these

Figure 3: Sixteen images obtained applying the Lee filter to the data shown in Figure 2.

estimators, the following biases were considered

$$D_1 = \frac{1}{N} \sum_{s_1=0}^{N-1} \sum_{s_2=0}^{N-1} \left(P_N(\sigma)(s_1, s_2) - S_\sigma(s_1, s_2) \right)$$

$$D_2 = \frac{1}{N} \sum_{s_1=0}^{N-1} \sum_{s_2=0}^{N-1} P_{N,T}(\sigma)(s_1, s_2) - S_\sigma(s_1, s_2)$$

$$D_3 = \frac{1}{N} \sum_{s_1=0}^{N-1} \sum_{s_2=0}^{N-1} P_{N,H}(\sigma)(s_1, s_2) - S_\sigma(s_1, s_2)$$

$$D_4 = \frac{1}{N} \sum_{s_1=0}^{N-1} \sum_{s_2=0}^{N-1} P_{N,F}(\sigma)(s_1, s_2) - S_\sigma(s_1, s_2)$$

over one thousand replications. These biases are referred to as D_i, and the value of the index denotes, respectively, the four estimators defined above.

The chosen period was $N = 32$, and the values $\nu \in \{0.5, 1, 1.5, 2\}$ and $\beta = 1$ were used. Also the considered number of looks were one and three, representing the image with the highest possible corruption by speckle ($n = 1$) and a signal-to-noise ratio usually found acceptable by remote sensing applications users ($n = 3$). The correlation lags $\ell \in \{2, 4, 8\}$ were chosen for the comparison of estimators.

The criteria chosen to make the comparison were based on an empiric rule (described in the following) and on the mean square error.

9.1 Empiric rule

This criterion is based on the assumption that the observed biases approximately obey a Gaussian distribution. Considering that an estimator is "admissible" when the sample confidence interval of the bias based on two standard deviations includes the zero value, the best estimator will be the admissible one which minimizes the variance. Tables 1, 2, 3, 4, 5, and 6 show the mean and standard deviations of the four aforementioned biases, and the acceptable estimators are highlighted, but in most of the studied cases most of the parameters values yielded no admissible estimators. Thus, we were induced to consider that the biases may be far from obeying the Gaussian law, and several boxplot and histograms were made in order to asses or discard this possibility. In figures 4 and 5, boxplots calculated with one thousand replications are shown, and it can be seen the strong asymmetry of the observed biases. This feature was observed in all the cases, even in those which led to admissible estimators. Hence, the essential condition in order to be able to use this criterion is to increase the period N in order to be able to use the central limit theorem.

9.2 Mean square error

Let E_i be the mean square error of the aforementioned biases, defined by

$$E_i = E(D_i^2) = E(D_i)^2 + Var(D_i) \qquad 1 \le i \le 4.$$

In the light of the asymmetries commented in the previous section, a more interesting criterion would be choosing as the best estimator the one having bias with minimum mean square error. Tables 1, 2, 3, 4, 5 and 6 also show the mean square error of the four biases and the best estimator was highlighted in boldface.

10 Conclusions

Several estimators for the spectrum were presented, and a Monte Carlo study was devised to compare four estimators in a variety of situations. Two criteria were considered in order to find the best estimator. The fist criterion is based on the assumption that the observed biases are approximately Gaussianly distributed, and it was clearly not true when the period was $N = 32$, thus no conclusion could be drawn. However, the situation could be very different working with periods like $N = 64$ or $N = 128$, because of the central limit theorem, but the computational cost should be taken in consideration. The second criterion was based on the mean square error of the biases and in this case, for one look images, the periodogram was the best among

$\nu = 0.5$ $\quad n = 1$			
$\ell = 2$			
	Mean	Std. Dev.	MSE
$\mathbf{D_1}$	-0.0005	0.0001	$3.e{-}7$
D_2	-0.0007	0.00003	$5.e{-}7$
D_3	-0.0007	0.00003	$5.e{-}7$
D_4	-0.0006	0.00004	$4.e{-}7$
$\ell = 4$			
	Mean	Std. Dev.	MSE
$\mathbf{D_1}$	-0.0005	0.0002	$3.e{-}7$
D_2	-0.0007	0.00006	$5.e{-}7$
D_3	-0.0007	0.00006	$5.e{-}7$
D_4	-0.0006	0.0001	$4.e{-}7$
$\ell = 8$			
	Mean	Std. Dev.	MSE
D_1	-0.0005	0.0005	$5.e{-}7$
D_2	-0.0007	0.0002	$5.e{-}7$
D_3	-0.0007	0.0002	$4.e{-}7$
$\mathbf{D_4}$	-0.0005	0.0004	$5.e{-}7$

Table 1: Mean, standard deviation and MSE between the truth and each estimator, with $n = 1$, $N = 32$ and $\beta = 1$.

$\nu = 2$ $\quad n = 1$			
$\ell = 2$			
	Mean	Std. Dev.	MSE
$\mathbf{D_1}$	-0.0043	0.0004	$2.e{-}5$
D_2	-0.0056	0.0001	$3.e{-}5$
D_3	-0.0056	0.0001	$3.e{-}5$
D_4	-0.0047	0.0003	$2.e{-}5$
$\ell = 4$			
	Mean	Std. Dev.	MSE
$\mathbf{D_1}$	-0.0042	0.0008	$2.e{-}5$
D_2	-0.0056	0.0002	$3.e{-}5$
D_3	-0.0056	0.0003	$3.e{-}5$
D_4	-0.0044	0.0007	$2.e{-}5$
$\ell = 8$			
	Mean	Std. Dev.	MSE
$\mathbf{D_1}$	-0.0039	0.0017	$2.e{-}5$
D_2	-0.0054	0.0005	$3.e{-}5$
D_3	-0.0054	0.0006	$3.e{-}5$
D_4	-0.0040	0.0017	$2.e{-}5$

Table 3: Mean, standard deviation and MSE between the truth and each estimator, with $n = 1$, $N = 32$ and $\beta = 1$.

$\nu = 1$ $\quad n = 1$			
$\ell = 2$			
	Mean	Std. Dev.	MSE
$\mathbf{D_1}$	-0.0014	0.0002	$2.e{-}6$
D_2	-0.0019	$6.e{-}5$	$3.e{-}6$
D_3	-0.0019	$6.e{-}5$	$3.e{-}6$
D_4	-0.0016	0.0001	$3.e{-}6$
$\ell = 4$			
	Mean	Std. Dev.	MSE
$\mathbf{D_1}$	-0.0014	0.0003	$2.e{-}6$
D_2	-0.0019	0.0001	$3.e{-}6$
D_3	-0.0018	0.0001	$3.e{-}6$
D_4	-0.0015	0.0002	$2.e{-}6$
$\ell = 8$			
	Mean	Std. Dev.	MSE
$\mathbf{D_1}$	-0.0013	0.0007	$2.e{-}6$
D_2	-0.0018	0.0003	$3.e{-}6$
D_3	-0.0018	0.0003	$3.e{-}6$
D_4	-0.0014	0.0006	$2.e{-}6$

Table 2: Mean, standard deviation and MSE between the truth and each estimator, with $n = 1$, $N = 32$ and $\beta = 1$.

$\nu = 0.5$ $\quad n = 3$			
$\ell = 2$			
	Mean	Std. Dev.	MSE
D_1	-0.0007	$1.e{-}5$	$5.e{-}7$
D_2	-0.0007	$4.e{-}6$	$5.e{-}7$
D_3	-0.0007	$4.e{-}6$	$5.e{-}7$
$\mathbf{D_4}$	-0.0006	$4.e{-}5$	$4.e{-}7$
$\ell = 4$			
	Mean	Std. Dev.	MSE
D_1	-0.0007	$2.e{-}5$	$5.e{-}7$
D_2	-0.0007	$8.e{-}6$	$5.e{-}7$
D_3	-0.0007	$9.e{-}6$	$5.e{-}7$
$\mathbf{D_4}$	-0.0006	0.0001	$4.e{-}7$
$\ell = 8$			
	Mean	Std. Dev.	MSE
D_1	0.0014	0.0038	$1.e{-}5$
$\mathbf{D_2}$	-0.0002	0.0013	$2.e{-}6$
D_3	-0.0002	0.0014	$2.e{-}6$
D_4	0.0164	0.0315	0.0012

Table 4: Mean, standard deviation and MSE between the truth and each estimator, with $n = 3$, $N = 32$ and $\beta = 1$.

$\nu = 1$		$n = 3$	
		$\ell = 2$	
	Mean	Std. Dev.	
D_1	-0.0018	$2.e{-}5$	$4.e{-}6$
D_2	-0.0019	$5.e{-}6$	$4.e{-}6$
D_3	-0.0019	$6.e{-}6$	$4.e{-}6$
$\mathbf{D_4}$	-0.0016	0.0001	$3.e{-}6$
		$\ell = 4$	
	Mean	Std. Dev.	MSE
D_1	-0.0019	$4.e{-}5$	$3.e{-}6$
D_2	-0.0019	$1.e{-}5$	$4.e{-}6$
D_3	-0.0019	$1.e{-}5$	$4.e{-}6$
$\mathbf{D_4}$	-0.0015	0.0002	$2.e{-}6$
		$\ell = 8$	
	Mean	Std. Dev.	MSE
D_1	0.0038	0.0067	$6.e{-}5$
$\mathbf{D_2}$	-0.0006	0.0024	$6.e{-}6$
D_3	-0.0005	0.0026	$7.e{-}6$
D_4	0.04585	0.0566	0.0053

Table 5: Mean, standard deviation and MSE between the truth and each estimator, with $n = 3$, $N = 32$ and $\beta = 1$.

Figure 4: Box plots for the $\nu = 2$, $\ell = 4$, $n = 1$, $N = 32$ situation.

$\nu = 2$		$n = 3$	
		$\ell = 2$	
	Mean	Std. Dev.	MSE
D_1	0.0074	0.0031	$6.e{-}5$
D_2	-0.0039	0.0009	$2.e{-}5$
$\mathbf{D_3}$	-0.0037	0.0010	$1.e{-}5$
D_4	0.0833	0.0202	0.0073
		$\ell = 4$	
	Mean	Std. Dev.	MSE
D_1	0.0085	0.0063	0.0001
D_2	-0.0033	0.0023	$2.e{-}5$
$\mathbf{D_3}$	-0.0031	0.0023	$1.e{-}5$
D_4	0.1036	0.0486	0.0131
		$\ell = 8$	
	Mean	Std. Dev.	MSE
D_1	0.0114	0.01408	0.0003
$\mathbf{D_2}$	-0.0019	0.0050	$3.e{-}5$
D_3	-0.0016	0.0052	$3.e{-}5$
D_4	0.1417	0.1203	0.0346

Table 6: Mean, standard deviation and MSE between the truth and each estimator, with $n = 3$, $N = 32$ and $\beta = 1$.
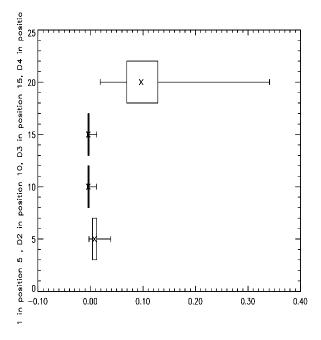

Figure 5: Box plots for the $\nu = 2$, $\ell = 4$, $n = 3$, $N = 32$ situation.

the considered estimators. When three looks data are available the choice was not so clear, because it depends on the correlation structure. The estimation with the Tuckey-Hanning was the best one when $\nu = 2$, but the pre-filtering was better in some other cases here considered.

This work will continue with the analysis of the $N = 64$ and $N = 128$ cases, and the proposal and assessment of robust estimation techniques. Another extension is the use of the Frost filter, that incorporates a correlation structure similar to the one here used.

Acknowledgments

References

[1] O.H. Bustos, A.G. Flesia (1998) Estimation of spectrum from speckled SAR images. *Proceedings of the second Latin-American Seminar on Radar Remote Sensing: Image Processing Techniques*, ESA SP 434, p. 61–65, European Space Agency (ESA), Santos, Brazil.

[2] A.C. Frery, H.-J. Müller, C.C.F. Yanasse, S.J.S. Sant'Anna (1997) A model for extremely heterogeneous clutter. *IEEE Transactions on Geoscience and Remote Sensing*, v. 35, p. 648–659.

[3] A.C. Frery, S.J.S. Sant'Anna, N.D.A. Mascarenhas, O.H. Bustos (1997), Robust inference techniques for speckle noise reduction in 1-look amplitude SAR images. *Applied Signal Processing*, v. 4, p. 61–76.

[4] X. Guyon (1991) *Random fields on a network: modeling, statistics, and applications*. Springer-Verlag, New York (Probability and its aplications).

[5] J.S. Lee (1986). Speckle suppression and analysis for synthetic aperture radar images, *Optical Engineering*, v. 25, p. 636–643.

[6] C.J. Oliver; S. Quegan (1998) *Understanding synthetic aperture radar images*. Artech House, Boston.

[7] G. Ronning (1977) A simple scheme for generating Multivariate Gamma distributions with non negative covariance matrix, *Technometrics*, v. 19, p. 179–183.

[8] M. Tur, K.C. Chin, and J.W. Goodman (1982) When is speckle noise multiplicative? *Appl. Opt*, v. 21, p. 1157–1159.

[9] C.C.F. Yanasse (1991). Statistical analysis of synthetic aperture radar images and its applications to system analysis and change detection. *PhD Thesis*. University of Sheffield, UK.

[10] C.C.F. Yanasse, A.C. Frery, S.J.S. Sant'Anna (1995) Stochastic distribution and multiplicative model: Relations, properties and applications to SAR Image Analysis, *Technical Report INPE-5630-NTC/318*. INPE, São José dos Campos, Brazil.